Concentration-Discharge Patterns Across the Gulf of Alaska Reveal Geomorphological and Glacierization Controls on Stream Water Solute Generation and Export

Jordan Jenckes[1], Daniel Enrique Ibarra[2], and Lee Ann Munk[3]

[1]University of Alaska Anchorage
[2]Brown University
[3]University of Alaska-Anchorage

November 22, 2022

Abstract

High latitude glacierized coastal catchments of the Gulf of Alaska (GoA) are undergoing rapid hydrologic changes in response to climate change and glacial recession. These catchments deliver important nutrients in the form of both inorganic and organic matter to the nearshore marine environment, yet are relatively understudied with respect to characterization of the solute generation processes and total yields. Using multiple linear regression informed by Bayesian Information Criterion analysis we empirically demonstrate how watershed characteristics affect solute generation as represented by concentration-discharge relationships. We find that watershed mean slope and relief control solute generation and that solute yields are influenced most by glacier coverage. We contribute a new flux and concentration-discharge based conceptualization for understanding solute cycles across a hydroclimatic gradient of GoA watersheds that can be used to better understand future watershed responses to rapid hydrologic change.

Concentration-Discharge Patterns Across the Gulf of Alaska Reveal Geomorphological and Glacierization Controls on Stream Water Solute Generation and Export

Jordan Jenckes[1,2] 0000-0002-1811-3076, **Daniel E. Ibarra**[3] 0000-0002-9980-4599, **Lee Ann Munk**[1] 0000-0003-2850-545X

[1]University of Alaska Anchorage, Department of Geological Sciences, Anchorage, Alaska 99508, USA

[2]University of Alaska Fairbanks, Department of Geosciences, Fairbanks, Alaska, 99775, USA

[3]Institute at Brown for Environment and Society and the Department of Earth, Environmental and Planetary Science, Brown University, Providence, Rhode Island 02912, USA

Corresponding author: Jordan Jenckes (jjenckes2@alaska.edu)

Key Points:

- Catchment glacial coverage controls annual solute yields consistent with the global trend in basins with similar glacier coverage.
- Watershed geomorphology has strong controls on concentration-discharge relationships.
- Solute yields are most significantly influenced by glacier coverage.

Abstract

High latitude glacierized coastal catchments of the Gulf of Alaska (GoA) are undergoing rapid hydrologic changes in response to climate change and glacial recession. These catchments deliver important nutrients in the form of both inorganic and organic matter to the nearshore marine environment, yet are relatively understudied with respect to characterization of the solute generation processes and total yields. Using multiple linear regression informed by Bayesian Information Criterion analysis we empirically demonstrate how watershed characteristics affect solute generation as represented by concentration-discharge relationships. We find that watershed mean slope and relief control solute generation and that solute yields are influenced most by glacier coverage. We contribute a new flux and concentration-discharge based conceptualization for understanding solute cycles across a hydroclimatic gradient of GoA watersheds that can be used to better understand future watershed responses to rapid hydrologic change.

Plain Language Summary

The Gulf of Alaska (GoA) region is experiencing rapid changes in climate causing glaciers to recede. Streams and rivers within basins that contain glaciers deliver vital nutrients to the ocean. However, regional studies to quantify the generation and delivery of rock-derived nutrients from watersheds to the ocean are lacking. This study uses statistical analysis to identify the mechanisms controlling the release of nutrients and to demonstrate the physical watershed characteristics that influence the flux of nutrients at the watershed scale. We find that topographic characteristics (slope and relief) control nutrient-generating processes and that glacier coverage is an important factor controlling the total amount of nutrients exported by streams. This contribution presents a new conceptualization for understanding nutrient delivery to the GoA that can be used to understand future responses to changing climate regimes.

1 Introduction

High latitude regions are warming at rates of two to three times the global average (IPCC, 2007). Precipitation regime changes associated with the increasing temperatures will result in increased precipitation, primarily in the form of autumn and winter rain (Beamer et al., 2017). Associated with these changes, global glacier volume will be 29-41% by 2100 compared to 2006 with a projected 20% decline of global glacier runoff (Radić et al., 2014). Ice fields and glaciers cover 18% of the 420,230 km^2 Gulf of Alaska (GoA) region and supply 47% of the freshwater water runoff (Neal et al., 2010). Looking to the future it is predicted that Alaska will experience a 30% decline in runoff by the end of the 21st century (Bliss et al., 2014) accompanied by a forecasted decrease of glacier volume between 32±11 and 58±14% for RCP2.6 and RCP8.5 respectively (Huss & Hock, 2015). As such, the climate change predicted for the 21st century will significantly alter the amount of freshwater discharging to the GoA along with changes in precipitation regimes. Currently, glacial fed streams have increased discharge and non-glacial fed streams have lower discharge. This paradigm will shift as coastal glacier coverage declines into the 21st century. Today, glaciers act as a control on seasonal runoff variation within a catchment. Stream discharge within a glacierized basin varies little year to year and peak runoff is generally predictable. Precipitation fed streams, conversely, have higher interannual variations in discharge due to their susceptibility to interannual climate variability. For example, Fountain and Tangborn (1985) suggest that basins with glacial coverage around

36% have the lowest year-to-year variation in discharge. Over the seasonal to monthly timescales, variations are at a maximum in July and August for basins with less than 10% glacier cover (Fountain & Tangborn, 1985).

Glaciers contain vast stores of water as ice and the seasonal discharge from meltwater to the GoA delivers freshwater and vital nutrients (Milner et al., 2017; Neal et al., 2010; O'Neel et al., 2015). The flux of nutrients to the nearshore environment sustains many trophic levels (Arimitsu et al., 2018). Therefore, previous studies focused on river chemistry of the GoA primarily investigate major nutrients N and P, dissolved organic carbon (DOC) and particulate organic carbon (POC) (Fellman et al., 2014; Hood et al., 2015, 2020; Hood & Berner, 2009). Past studies of micronutrients have focused on Al concentration in river plumes in the GoA (Brown et al., 2010) and Fe fluxes in glacierized and non-glacierized tributaries feeding the Copper River (Schroth et al., 2011). Brennan et al. (2014) examined grab samples of 61 streams across Alaska (13 from within the GoA region) for radiogenic Sr isotope ratios and concentrations of major cations, with the goal of broadly illustrating patterns in Sr isotope ratios and carbonate vs. silicate weathering. However, there remains a conspicuous lack of work examining the hydrogeochemical cycles of major elements, anions and micronutrients such as silica. Analysis of the major elements and anions in stream water can be used to reveal hydrologic properties within watersheds (Godsey et al., 2009). Additionally, investigating major element and anion concentrations may offer further insights into carbon cycling (Amiotte Suchet & Probst, 1993; A. F. White & Blum, 1995), chemical weathering-climate feedback (Eiriksdottir et al., 2013); and, specifically within the context of the GoA, how glacial coverage within a watershed affects physical and chemical weathering (Anderson, 2005; Sharp et al., 1995; Torres et al., 2017).

The chemical composition of glacier fed streams is distinct compared to non-glacier fed streams. Primarily, glacial melt runoff contains more K^+ and less Si compared to average global rivers (Anderson et al., 1997). The dominant ions within glacial fed streams are Ca^{2+}, HCO_3^-, and SO_4^{2-} with high Ca^{2+}:Si and low HCO_3^-: SO_4^{2-} (Tranter & Wadham, 2003). The major cation composition of glacier runoff is always Ca^{2+}, controlled by the dissolution kinetics of carbonates, which are found within most bedrock (Raiswell, 1984). Further, specific discharge is a primary control on area-normalized weathering rates (yields) globally (Anderson et al., 1997; Maher & Chamberlain, 2014; Torres et al., 2017).

Rates of weathering, and both solute generation and flux, especially within glacierized catchments, are primarily controlled by stream discharge (Rose et al., 2018). Dilution curves, or concentration discharge (C-Q) relationships, are derived using a power law in the form of $C=aQ^b$, where C is concentration, Q is discharge, and a and b are constants (Johnson et al., 1969). Different elements exhibit varying responses to increases in discharge (Godsey et al., 2009; Ibarra et al., 2016; Moon et al., 2014); this relationship is an important descriptor of the mechanisms controlling solute flux and weathering within a watershed. C-Q relationships can aid in elucidating future physical and chemical weathering regimes within the GoA watersheds which is particularly relevant under the current climate trajectory and projections of glacial recession because of more precipitation occurring as rain and increased air temperatures.

In this contribution we use physical watershed characteristics and USGS legacy water chemistry and discharge data from streams sites across the GoA to investigate how watershed characteristics affect solute yields and C-Q relationships. We explore the dissolved and suspended loads across stream sites to elucidate physical and chemical weathering patterns in the GoA. Additionally, we broadly show dominant weathering regimes and primary sources of solutes provided to stream water. This analysis is a unique approach to describe and explore controls on the generation and yields of solutes across the GoA.

2 Study Area and Methods

2.1 Gulf of Alaska Region

The GoA watershed (Figure 1a.) and the seven sub-regions span a perhumid hydroclimate in the Southeast, to a subarctic hydroclimate in the northern regions. Precipitation varies considerably on a seasonal basis and across the region. Seasonal precipitation (Thornton et al., 2020) for the major regions of the GoA are shown in Figure 1c. The majority of precipitation occurs in the fall and winter with the Southeast, Central Coast and Prince William Sound regions receiving far greater precipitation than other regions. This is driven by orographic precipitation and primary storm track trajectories. Regions on the lee of the coastal ranges, Copper River, Knik Arm/Kenai Peninsula and Susitna River, receive far less precipitation compared to the windward. The glaciers of the GoA region occur primarily near the coast, however large glaciers also exist within the interior northern reaches of the Susitna and Copper River regions (Figure 1b).

2.2 Stream Sites and Watersheds

The USGS NWIS was queried to obtain all stream sites within Alaska that contain water chemistry analysis. We then spatially filtered the dataset to find stream sites that drain into the GoA. Each stream site was further spatially filtered and assigned a region based on the seven defined regions (Figure 1a). The stream sites contained within the GoA were filtered to those sites that have total dissolved solute (TDS) and total suspended sediment (TSS) paired with stream discharge. To explore concentration-discharge relationships we chose stream sites that have at least 12 paired concentration and discharge measurements for HCO_3^-, Ca^{2+}, Mg^{2+}, Na* (Cl-corrected; Ibarra et al., 2016; Moon et al., 2014), K^+, SO_4^{2-}, SiO_2 and TSS resulting in 34 stream sites total that fit our criteria. For watershed boundaries of the 34 stream sites with requisite C-Q data we use the watersheds delineated by Curran and Biles (2020).

2.3 Watershed characteristics

We calculated physical and climate watershed characteristics based on five separate datasets: landcover (CCRS, 2015), geology (Garrity & Soller, 2009), elevation statistics (Tadono et al., 2014), glacial coverage (RGI Consortium, 2017) and climate (Thornton et al., 2020). Each dataset was clipped using watershed boundaries and the specific parameters were grouped and calculated. A full description of the watershed characteristics and analysis is available in the supporting information (Text S1).

2.4 Weathering Regimes

We broadly investigate physical and chemical weathering regimes within watersheds of GoA by exploring the yield of TDS and TSS and the HCO_3^-:SiO_2. Because we do not correct our data for rainfall contributions or carbonate weathering the TDS:TSS relationship illustrates a relative weathering index (RWI). For the calculation of TDS, we summed concentrations of Ca^{2+}, Mg^{2+}, Na^+, K^+, and SiO_2. We compare mean TDS and TSS yields of global rivers (Gaillardet et al., 1999) along with the mean TDS and TSS yields of the GoA streams. Similarly, we show all

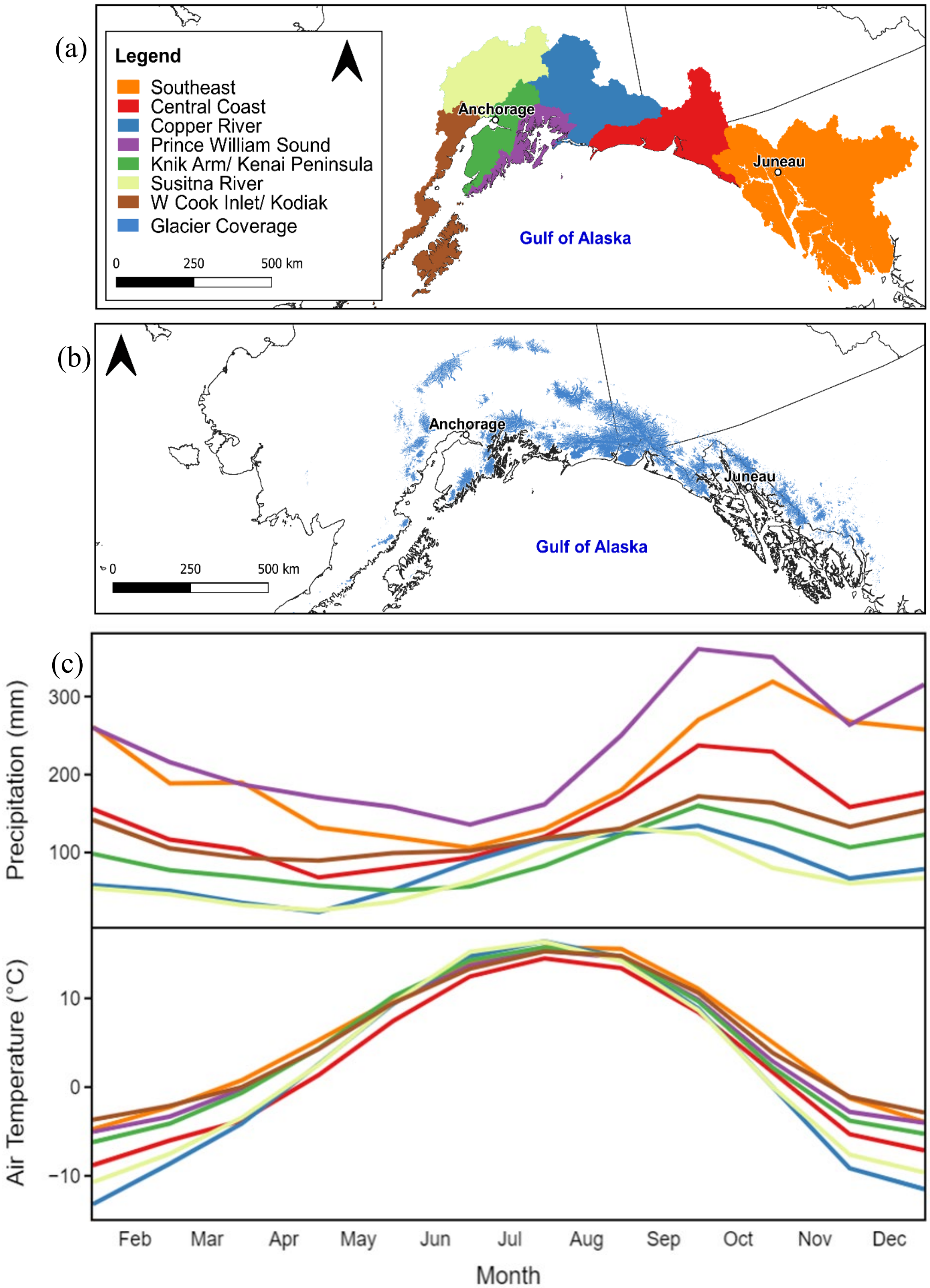

Figure 1. Regions of the Gulf of Alaska (a), regional glacier coverage (b), and associated monthly mean precipitation and air temperature (c). The coastal regions of Prince William Sound, Southeast and Central Coast receive the greatest amount of precipitation. Mean summer air temperatures across regions are similar while mean air temperature of the Copper River and the Susitna River regions are notably colder that the other regions.

147

available [HCO_3^-]:[SiO_2] for the GoA streams and the mean [HCO_3^-] and [SiO_2] with global rivers for comparison. For this study we do not correct for rainwater contribution because our main objective is to investigate solute generation and yields and to broadly appropriate sources of solutes.

2.5 Solute Yield and C-Q Relationships

We calculate solute yields by multiplying the solute concentrations by the instantaneous discharge measurements and dividing by the watershed area. Where we present mean yield values for each stream we first calculate the yields for each measurement and calculate the mean of each calculated yield value at each stream site.

To explore C-Q relationships we fit the chemistry and discharge data of the 34 sites to the power law function $C=aQ^b$ ('nls2' R package, Grothendieck, 2013; following code modified from Ibarra et al., 2016, 2017 and Wymore et al., 2017) where C is the concentration, Q is discharge and a and b are constants. The value of *b* (the power law exponent or *b*-value), in logC-logQ space, is the slope of the resulting linear fit. The slope of the line (*b*-value) has a physical interpretation (Godsey et al., 2009). Slopes near -1 indicate simple dilution, and that concentration varies inversely with discharge. A slope around zero (typically -0.1 to +0.1) indicates chemostatic behavior within a watershed, meaning, as discharge increases the concentration remains relatively unchanged. Power law exponents greater than zero indicate enrichment of a solute as discharge increase. We calculated fits for HCO_3^-, Ca^{2+}, Mg^{2+}, Na*, K^+, SO_4^{2-}, SiO_2 and TSS. However, we do not use the *b*-values for K^+ and SO_4^{2-} in further analysis due to the poor quality of the modeled fits.

2.6 Statistical Analysis

To determine the relationships between physical watershed characteristics, solute yields, and C-Q relationships we use Bayesian Information Criterion (BIC) to select the minimum number of watershed characteristics that will best describe the variation in a solute yield or the power law exponent. Each of the physical and climate-based watershed characteristics within Table S2 were used in the BIC analysis. We then use the minimum numbers of parameters selected by the BIC in a multiple linear regression model to find how well the parameters describe the variation in solute yields and *b*-values. For each parameter used in the linear regression we show whether the solute yield or *b*-value is positively or negatively related and if the derived slope with respect to a given parameter is statistically significant ($p<0.05$).

3 Results and Discussion

3.1 Solute C-Q Relationships

On a regional basis streams draining to the GoA exhibit variable C-Q relationships. The C-Q relationships of HCO_3^-, Ca^{2+}, and SiO_2 are used as representative solutes for rock-derived nutrients (Figure 2). The C-Q relationships of the solutes across the regions may be influenced by climate regimes (Godsey et al., 2019), lithology (Ibarra et al., 2016), geomorphology (Torres et al., 2015) and vegetation (Wymore et al., 2017). Median *b*-values at a regional level for HCO_3^-, Ca^{2+}, and SiO_2 range from -0.23 – 0.01, -0.24 – -0.07, and -0.25 – -0.11 respectively (Table S2). The Southeast and Susitna River regions have the lowest median *b*-values, and the W. Cook Inlet/Kodiak region has the highest median *b*-values. Basins within the Susitna River region have

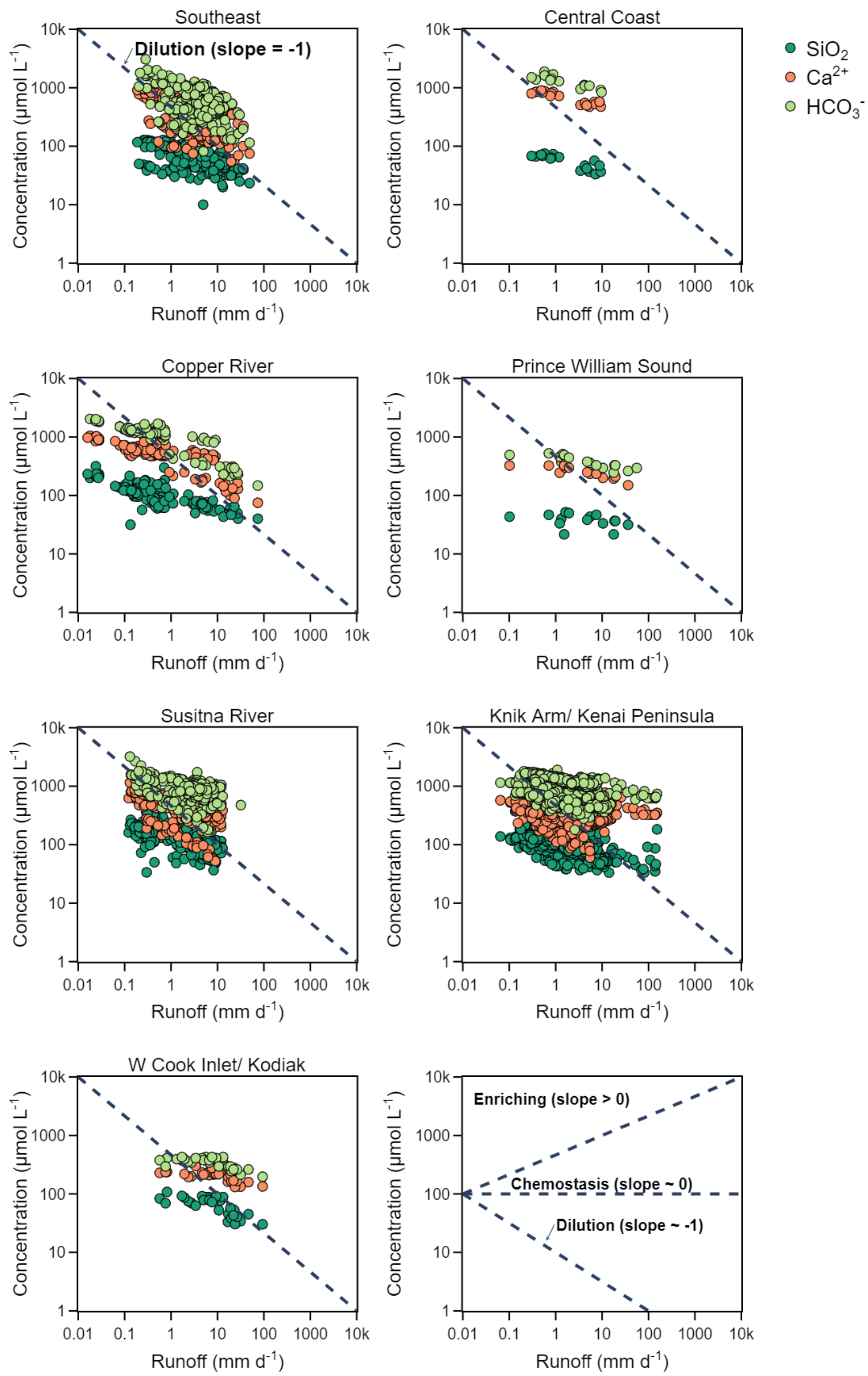

Figure 2. Concentration-discharge relationships for SiO_2, Ca^{2+}, and HCO_3^- for each of the seven regions of the GoA. An example plot (lower right) illustrates the physical interpretation of a given C-Q slope. Streams within the GoA region do not conform to simple dilution behavior based on intermediate slopes. This indicates that streams throughout the GoA behave similarly to streams within the conterminous United States (e.g. Godsey et al., 2009) why do we make this comparison here? All other comparisons are to global rivers. Regional difference of C-Q relationships may indicate different controls such as hydroclimate and geomorphology.

189

shallow slopes which may contribute to the lower overall *b*-values (e.g. Torres et al., 2015; discussed further below). In the Southeast region the basins receive a greater amount of annual precipitation, which may contribute to high mean specific discharge leading to lower *b*-values (e.g. Godsey et al., 2009, 2019). Within the W. Cook Inlet/Kodiak region the basins are relatively steep with high relief which may contribute to the higher observed *b*-values. Additionally, because historical USGS sampling efforts do not generally capture the highest discharge events, the available dataset is likely biased such that overall C-Q relationships may appear to be more chemostatic than if higher discharge events were more represented.

3.2 Weathering Regimes

Gulf of Alaska streams span a large range in dissolved solute and sediment yields. Figure 3a illustrates the TDS and TSS data for 34 of the GoA streams, with linear lines indicating the ratio of the load being exported in the dissolved phase vs. the suspended phase. The RWI describes the ratio between TDS and TSS yields that are not corrected for carbonate dissolution and represents the partitioning of landscape denudation into chemical vs. physical weathering, which on long timescales, at steady state, is set by the uplift rate (eg., (Dixon and von Blanckenburg, 2012; Gabet and Mudd, 2009; Hilley et al., 2010; Maher and Chamberlain, 2014; Waldbauer and Chamberlain, 2005). For example, in Figure 3a points plotting above the 0.75 line instantaneously export a majority (i.e., 75%) of the load as dissolved solids. Points plotting below the 0.1 line export a majority of the load as suspended sediment. Importantly, points plotting below 0.5 have lower inferred chemical weathering compared to physical weathering. Erosion by glaciers combined with steep topography produces enhanced physical weathering in the GoA watersheds. However, at a given erosion rate, chemical weathering is on average lower within catchments of the GoA compared to global rivers.

Mean TDS and TSS yield ratios of the selected streams of GoA are lower in overall fluxes (area-normalized) than many of the global rivers (Figure 3b). Compared to other northern high latitude rivers (Ob, Kuskokwim, Yukon, and Mackenzie) within the global dataset the GoA streams have similar RWI values. Globally, the suspended load of rivers dominates the material flux to the oceans (Walling & Webb, 1983). A positive trend between dissolved and suspended load exists, however a clear relationship is not systematic (Walling & Webb, 1983). Suspended sediment loads have been shown to have a negative relationship with basin area, a trend not shared by the dissolved load. Within the GoA dataset, and most notably within the Southeast region (Figure 3a-b), streams near the RWI = 0.1 line are generally the glacierized basins and streams near and above the RWI = 0.75 are non-glacierized (Figure 3b). Chemical weathering is limited within glacierized basins though there is an increase in physical erosion. We infer that increased generation of fresh mineral surfaces within glacierized basins is being outpaced by the time (i.e., kinetics) required for chemical weathering reactions to occur (Ferrier & Kirchner, 2008; Torres et al., 2017).

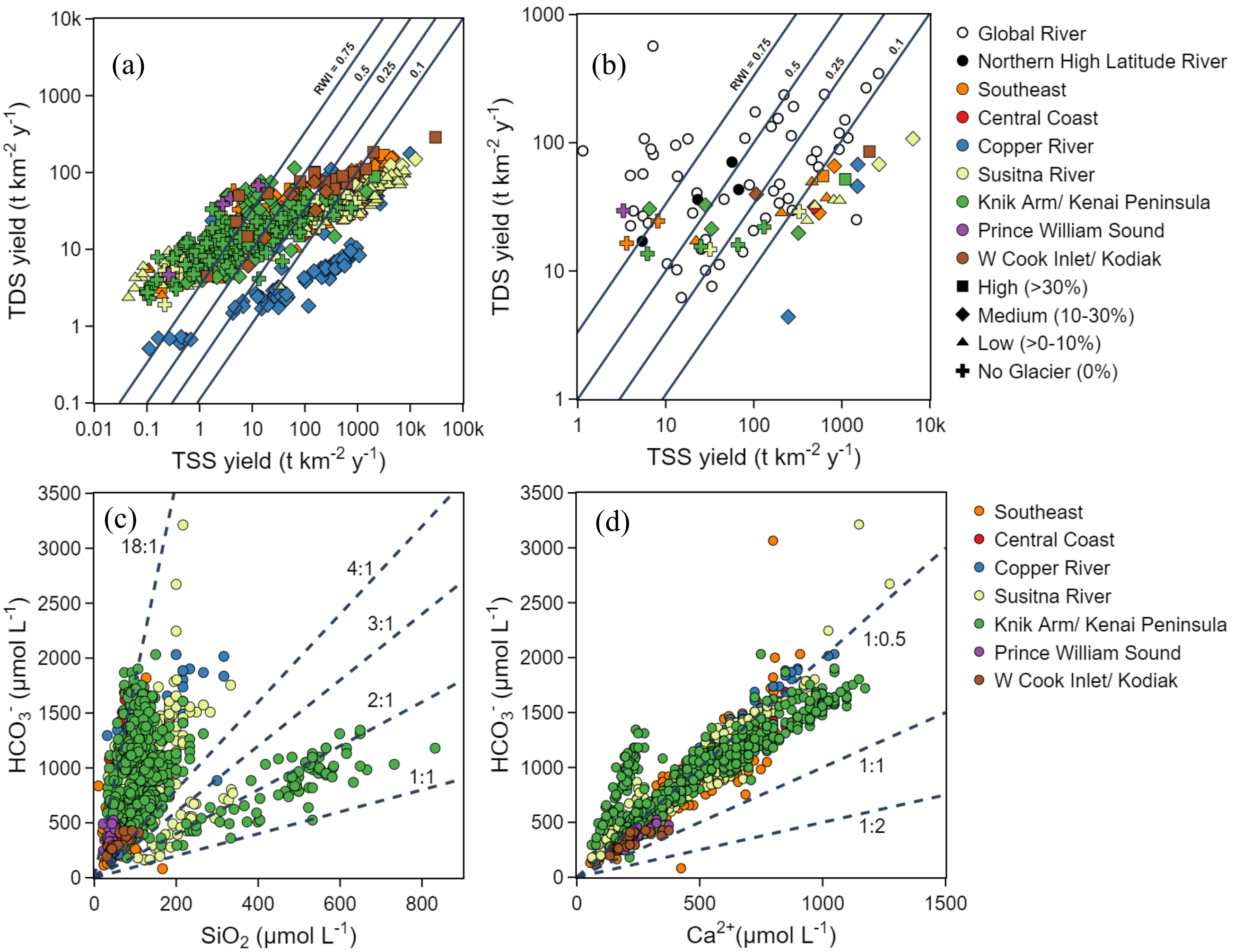

Figure 3. TDS yield and TSS yield for all GoA sites with available data (a). Mean TDS and TSS yields for each stream site with data from global rivers (Gaillardet et al., 1999) (b). Symbols indicate the range of percent glacier coverage within each watershed. Watersheds with medium to high glacier coverage generally plot below the RWI = 0.1 implying that chemical weathering within moderately to highly glacierized catchments is relatively lower compared to physical weathering. Concentration of HCO_3^- vs. SiO_2 for GoA stream sites (c). Three streams plot on or below the 2:1 line indicating that silicates are the primary weathering minerals. The rest of the streams plot above the 4:1 line suggesting carbonates as the primary weathering minerals. HCO_3^- vs. Ca^{2+} concentration this is oppositely stated in the SI (d) for streams primarily plot near the 1:0.5 line indicating carbonate dissolution by carbonic acid.

Bicarbonate and SiO_2 concentration ratios provide a mechanism to investigate the dominant chemical weathering sources within a basin at a broad scale. The GoA streams are dominated by high HCO_3^-:SiO_2 values (Figure 3c). Carbonate dissolution supplies the majority of ions to the dissolved load compared to silicate weathering regardless of primary bedrock lithology (Raiswell, 1984). Two non-glacial fed streams in the Knik Arm/Kenai Peninsula region and one non-glacial fed stream in the Susitna River region, are primarily influenced by silicate weathering (based on the dominant bedrock geology of these catchments; Table S2) with HCO_3^-:SiO_2 values near 2:1, typical HCO_3^-:SiO_2 of silicate net weathering reactions range from <1:1 to 4:1 (e.g., Bouchez and Gaillardet, 2014; Ibarra et al., 2016; Maher, 2011; Winnick and Maher, 2018). Furthermore, the ratio between HCO_3^- and Ca^{2+}, illustrated in Figure 3d, is consistent with dissolution of carbonate by carbonation (Equation S1). Within glacierized basins the lithology is a secondary control on the chemical composition of stream water (Raiswell, 1984; White et al., 2001). Further, decreased temperatures within glacierized basins reduce silicate-weathering rates (Anderson, 2005). Additionally, silicate denudation rates in glacierized basins are lower compared to non-glacierized basins at similar specific discharge values (Anderson et al., 1997). Therefore, glacierized basins within the GoA do not export more area normalized SiO_2 compared to non-glacierized basins.

Compared to mean global values, the streams of the GoA generally have lower mean HCO_3^-:SiO_2 (Figure S5). Mean HCO_3^-:SiO_2 values for high latitude northern rivers are also slightly elevated compared to GoA streams. We speculate that this could be driven by one of two factors. First, a lack of monolithologic carbonate catchments in the GoA. Second, lower overall primary productivity (due to colder temperatures and shorter growing season), leading to reduced soil CO_2 values and thus less HCO_3^- generation thereby lowering the HCO_3^-:SiO_2 values (all else being equal) (Raymond & Cole, 2003).

3.4 Geomorphology and Glacier Coverage

To explore controls on the above observations we rely on our BIC analysis. We find through BIC and multiple linear regression that solute yields are controlled by glacier coverage while C-Q relationships are primarily controlled by watershed geomorphology (Table S1). Earlier efforts have linked watershed geomorphology and C-Q relationships, suggesting the differences in transport vs. supply regimes are controlled by changes in fluid-residence times in the weathering zone (Maher, 2011; Maher & Chamberlain, 2014; McGuire et al., 2005; Torres et al., 2015). For example, we find that *b*-values for HCO_3^-, Ca^{2+}, and SiO_2 and watershed slope are positively correlated (Figure 4a). Fluid transit time distributions within watersheds with steeper topography are likely greater than watersheds with shallower slopes. Longer transit times may allow the concentration of the solutes to reach equilibrium with respect to the net weathering reactions (Maher, 2011; Maher & Chamberlain, 2014; Torres et al., 2015). The BIC analysis only identified glacier coverage as an important parameter with respect to the *b*-value for SiO_2. Figure 4b illustrates the relationship between *b*-values and glacier coverage. We find this relationship to be undefined, however, there are some surprising observations. The median *b*-values for HCO_3^-, Ca^{2+}, and SiO_2 of the glacier fed streams are -0.15, -0.19, -0.19 respectively, indicating solute concentrations are not significantly affected by changes in discharge (area-normalized). Further, there are several glacier fed streams in our dataset that exhibit at or near chemostatic behavior (*b*-values between -0.1 and 0.1) (e.g., Hindshaw et al., 2011, 2014).

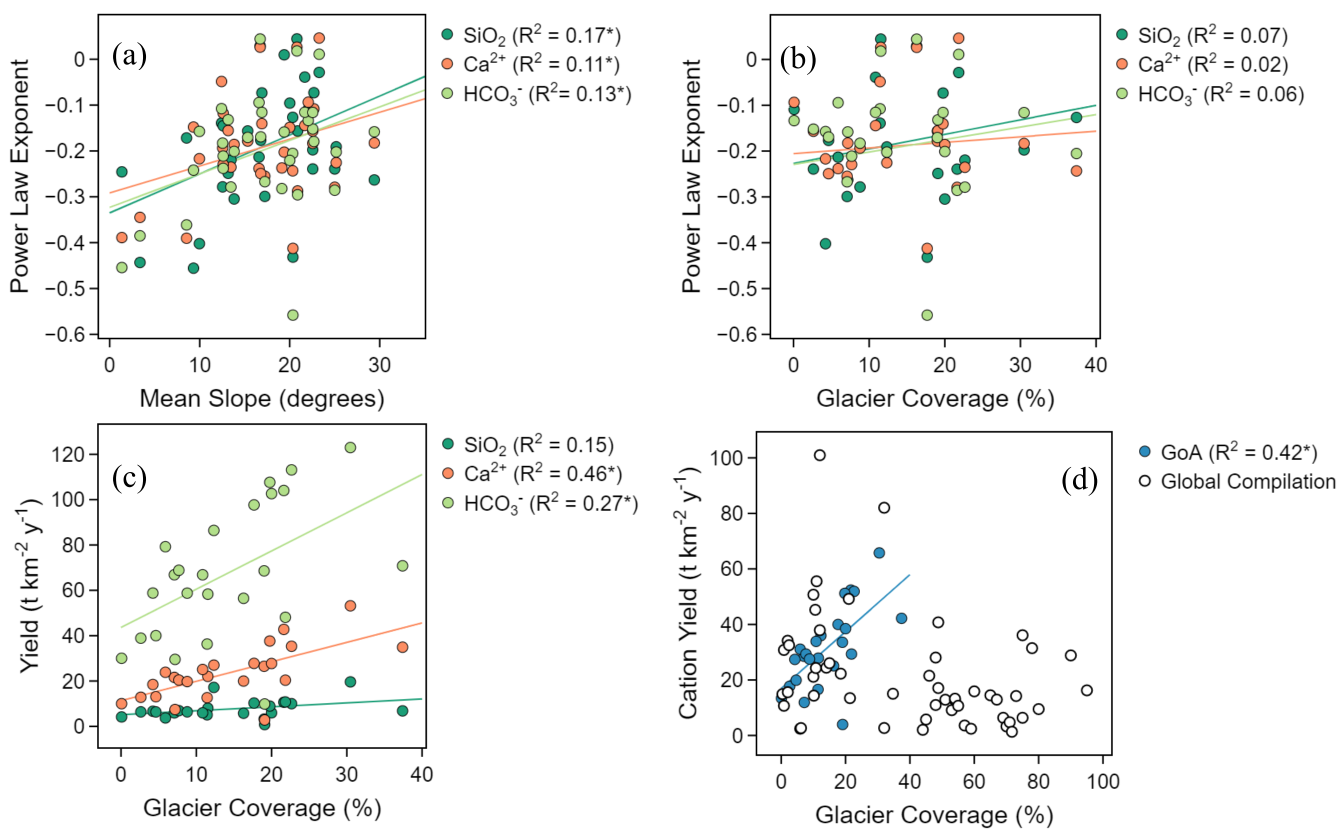

Figure 4. Relationship between power law exponents and mean catchment slope (a) and glacier coverages (b) for SiO_2, Ca^{2+}, and HCO_3^-. Mean slope is used as an example geomorphic parameter. The *b*-values for SiO_2, Ca^{2+}, and HCO_3^- show a positive relationship with mean slope, while there is no relationship of these *b*-values and glacier coverage. However, calculated yields for SiO_2, Ca^{2+}, and HCO_3^-. vs. glacier coverage (c) show a positive relationship. Cation yields vs. glacier coverage (d) for the GoA streams with data compiled by Torres et al. (2017) for glacierized watersheds globally. These results indicate that to a certain extent, glaciers affect the solute yield, while watershed slope (and other geomorphic characteristics) control solute generation. Asterisks next to R^2 value denotes where $p < 0.05$.

Broadly, the patterns in C-Q relationships within the glacierized basins generally conform to observations in non-glacier fed systems (e.g. Godsey et al., 2009).

Figure 4c illustrates the relationship between the yield of SiO_2, Ca^{2+}, and HCO_3^- and glacier coverage. The yield of these weathering derived solutes exhibits positive relationships with glacier coverage. Previous work examining weathering rates versus watershed glacier coverage showed a negative relationship across a global dataset (Torres et al., 2017). Within the GoA dataset, glacier coverages range from 0% to 40%, while the dataset presented by Torres et al. (2017) ranges from 0% to 95% (Figure 4d). Cation yields within glacierized basins of the GoA have a distinct positive relationship with glacier coverage (Figure 4d). Though we do not derive a relationship for the globally derived dataset, we propose that there may be two distinct trends when examining the cation yield vs. glacier coverage relationship. A threshold appears to exist at glacier coverages < 35-40% in which a positive relationship exists between cation yields and glacier coverage. Basins with >40% glacier coverage may have a slight negative relationship between cation yields and glacier coverage (and drives the relationship fit to the dataset by Torres et al., 2017; their Figure 1b). We suggest that the proportionally small area of proglacial environments in these catchments may be a limiting factor for solute generation in basins with high glacier coverage. As such, proglacial environments may be an important driver of continued weathering (Deuerling et al., 2017). Additionally, the lithology of the GoA watershed may contribute to the strong positive relationship observed between cation yields and glacier coverage. Metasedimentary rocks that are highly fractured are more easily weathered compared to granite or basalt bedrock (Bluth & Kump, 1994). Furthermore, future work is needed to partition solutes into specific lithologic source components (e.g. an inverse weathering model; Gaillardet et al., 1999). This will aid in further elucidating how modifications in the physical watershed characteristics due to glacial recession may alter fluxes of critical nutrients to the GoA.

4 Conclusions

We find that TDS and TSS yields of streams in the GoA cover a large range of values, implying variable rates of chemical and physical weathering, and variable partitioning of overall denudation. Streams fed by glaciers tend to have lower chemical weathering with higher amounts of physical weathering (lower RWI values). Conversely, streams with low to no glacier coverage have higher RWI values. In terms of dominant weathering regimes, carbonate dissolution provides the majority of solutes to streams in the GoA regardless of dominant lithology.

Based on our statistical analysis of solute yields, C-Q relationships, climate, and physical watershed characteristics we find that geomorphology and glacier coverage affect the yields and solute generation differently. Power law exponents are primarily explained by geomorphology-related landscape characteristics such as slope, elevation, and aspect. We infer that water transit times are the primary control on solute generation and influence the observed C-Q relationships (Torres et al., 2015). Solute yields on the other hand are controlled by the amount of glacier coverage within a catchment. This is unsurprising given that glaciers are a primary control on stream runoff within a given catchment (Fleming, 2005; Fountain & Tangborn, 1985) and that most solute yields increase with increases in runoff. However, a novel result of this work is that we demonstrate that physical watershed characteristics control solute generation (C-Q relationships) and glacier coverage control area normalized fluxes (yields). This new conceptualization for understanding solute delivery to the GoA indicates that glaciers ultimately control the absolute amount of solutes exported to the ocean due to runoff generation, however downstream characteristics control the generation of solutes displayed in C-Q patterns. Future work will need to aim at estimating annual fluxes of solutes and to forecast how solute yields and fluxes may change as glaciers continue to rapidly recede in the coming century.

Acknowledgments

The authors would like to thank Janet Curran of the USGS for providing watershed boundaries for this study. Funding for this research is provided by NSF award OIA-1757347 to Lee Ann Munk and others. Jordan Jenckes received support from the Sloan Indigenous Graduate Partnership Fellowship. Daniel E. Ibarra was funded by the UC Berkeley Miller Institute and UC President's Postdoctoral Fellowship. The authors declare no competing interests.

Data Availability

Data used in this manuscript will be made available by doi on https://scholarworks.alaska.edu/. All data are now available in the supporting information document provided with this manuscript.

References

Amiotte Suchet, P., & Probst, J. L. (1993). Modelling of atmospheric CO2 consumption by chemical weathering of rocks: Application to the Garonne, Congo and Amazon basins. *Chemical Geology*, *107*(3–4), 205–210. https://doi.org/10.1016/0009-2541(93)90174-H

Anderson, S. P. (2005). Glaciers show direct linkage between erosion rate and chemical weathering fluxes. *Geomorphology*, *67*(1-2 SPEC. ISS.), 147–157. https://doi.org/10.1016/j.geomorph.2004.07.010

Anderson, S. P., Drever, J. I., & Humphrey, N. F. (1997). Chemical weathering in glacial environments. *Geology*, *25*(5), 399–402. https://doi.org/10.1130/0091-7613(1997)025<0399:CWIGE>2.3.CO

Arimitsu, M. L., Hobson, K. A., Webber, D. N., Piatt, J. F., Hood, E. W., & Fellman, J. B. (2018). Tracing biogeochemical subsidies from glacier runoff into Alaska's coastal marine food webs. *Global Change Biology*, *24*(1), 387–398. https://doi.org/10.1111/gcb.13875

Beamer, J. P., Hill, D. F., McGrath, D., Arendt, A., & Kienholz, C. (2017). Hydrologic impacts of changes in climate and glacier extent in the Gulf of Alaska watershed. *Water Resources Research*, *53*(9), 7502–7520. https://doi.org/10.1002/2016WR020033

Bliss, A., Hock, R., & Radić, V. (2014). Global response of glacier runoff to twenty-first century climate change. *Journal of Geophysical Research: Earth Surface*, *119*(4), 717–730. https://doi.org/10.1002/2013JF002931

Bluth, G. J. S., & Kump, L. R. (1994). Lithologic and climatologic controls of river chemistry. *Geochimica et Cosmochimica Acta*, *58*(10), 2341–2359. https://doi.org/10.1016/0016-7037(94)90015-9

Bouchez, J., & Gaillardet, J. (2014). How accurate are rivers as gauges of chemical denudation of the Earth surface? *Geology*, *42*(2), 171–174. https://doi.org/10.1130/G34934.1

Brennan, S. R., Fernandez, D. P., Mackey, G., Cerling, T. E., Bataille, C. P., Bowen, G. J., & Wooller, M. J. (2014). Strontium isotope variation and carbonate versus silicate weathering in rivers from across Alaska: Implications for provenance studies. *Chemical Geology*, *389*, 167–181. https://doi.org/10.1016/j.chemgeo.2014.08.018

Brown, M. T., Lippiatt, S. M., & Bruland, K. W. (2010). Dissolved aluminum, particulate aluminum, and silicic acid in northern Gulf of Alaska coastal waters: Glacial/riverine inputs and extreme reactivity. *Marine Chemistry*, *122*(1–4), 160–175. https://doi.org/10.1016/j.marchem.2010.04.002

CCRS. (2015). 2015 Land Cover of North America at 30 meters. http://www.cec.org/nalcms

Curran, J. H., & Biles, F. E. (2020). Identification of Seasonal Streamflow Regimes and Streamflow Drivers for Daily and Peak Flows in Alaska. *Water Resources Research*. https://doi.org/10.1029/2020wr028425

Deuerling, K. M., Martin, J. B., Martin, E. E., & Scribner, C. A. (2017). Hydrologic exchange and chemical weathering in a proglacial watershed near Kangerlussuaq, west Greenland. https://doi.org/10.1016/j.jhydrol.2017.11.002

Dixon, J. L., & von Blanckenburg, F. (2012). Soils as pacemakers and limiters of global silicate weathering. *Comptes Rendus - Geoscience*, *344*(11–12), 597–609. https://doi.org/10.1016/j.crte.2012.10.012

Eiriksdottir, E. S., Gislason, S. R., & Oelkers, E. H. (2013). Does temperature or runoff control the feedback between chemical denudation and climate? Insights from NE Iceland. *Geochimica et Cosmochimica Acta*, *107*, 65–81. https://doi.org/10.1016/j.gca.2012.12.034

Fellman, J. B., Hood, E., Spencer, R. G. M., Stubbins, A., & Raymond, P. A. (2014). Watershed Glacier Coverage Influences Dissolved Organic Matter Biogeochemistry in Coastal Watersheds of Southeast Alaska. *Ecosystems*, *17*(6), 1014–1025. https://doi.org/10.1007/s10021-014-9777-1

Ferrier, K. L., & Kirchner, J. W. (2008). Effects of physical erosion on chemical denudation rates: A numerical modeling study of soil-mantled hillslopes. *Earth and Planetary Science Letters*, *272*(3–4), 591–599. https://doi.org/10.1016/j.epsl.2008.05.024

Fleming, S. W. (2005). Comparative analysis of glacial and nival streamflow regimes with implications for lotic habitat quantity and fish species richness. *River Research and Applications*, *21*(4), 363–379. https://doi.org/10.1002/rra.810

Fountain, A. G., & Tangborn, W. V. (1985). The Effect of Glaciers on Streamflow Variations. *Water Resources Research*, *21*(4), 579–586. https://doi.org/10.1029/WR021i004p00579

Gabet, E. J., & Mudd, S. M. (2009). A theoretical model coupling chemical weathering rates with denudation rates. *Geology*, *37*(2), 151–154. https://doi.org/10.1130/G25270A.1

Gaillardet, J., Dupre, B., Louvat, P., & Allegre, C. J. (1999). *Global silicate weathering and CO consumption rates deduced 2 from the chemistry of large rivers*. *Chemical Geology* (Vol. 159).

Godsey, S. E., Kirchner, J. W., & Clow, D. W. (2009). Concentration-discharge relationships reflect chemostatic characteristics of US catchments. *Hydrological Processes*, *23*(13), 1844–1864. https://doi.org/10.1002/hyp.7315

Godsey, S. E., Hartmann, J., & Kirchner, J. W. (2019). Catchment chemostasis revisited: Water quality responds differently to variations in weather and climate. *Hydrological Processes*, *33*(24), 3056–3069. https://doi.org/10.1002/hyp.13554

Hilley, G. E., Chamberlain, C. P., Moon, S., Porder, S., & Willett, S. D. (2010). Competition between erosion and reaction kinetics in controlling silicate-weathering rates. *Earth and Planetary Science Letters*, *293*(1–2), 191–199. https://doi.org/10.1016/j.epsl.2010.01.008

Hindshaw, R. S., Tipper, E. T., Reynolds, B. C., Lemarchand, E., Wiederhold, J. G., Magnusson, J., et al. (2011). Hydrological control of stream water chemistry in a glacial catchment (Damma Glacier, Switzerland). *Chemical Geology*, *285*(1–4), 215–230. https://doi.org/10.1016/j.chemgeo.2011.04.012

Hindshaw, R. S., Rickli, J., Leuthold, J., Wadham, J., & Bourdon, B. (2014). Identifying weathering sources and processes in an outlet glacier of the Greenland Ice Sheet using Ca and Sr isotope ratios. *Geochimica et Cosmochimica Acta*, *145*, 50–71. https://doi.org/10.1016/j.gca.2014.09.016

Hood, E., & Berner, L. (2009). Effects of changing glacial coverage on the physical and biogeochemical properties of coastal streams in southeastern Alaska. *Journal of Geophysical Research: Biogeosciences*, *114*(3), 1–10. https://doi.org/10.1029/2009JG000971

Hood, E., Battin, T. J., Fellman, J., O'neel, S., & Spencer, R. G. M. (2015). Storage and release of organic carbon from glaciers and ice sheets. *Nature Geoscience*, *8*(2), 91–96. https://doi.org/10.1038/ngeo2331

Hood, E., Fellman, J. B., & Spencer, R. G. M. (2020). Glacier Loss Impacts Riverine Organic Carbon Transport to the Ocean. *Geophysical Research Letters*, *47*(19), 1–9. https://doi.org/10.1029/2020GL089804

Huss, M., & Hock, R. (2015). A new model for global glacier change and sea-level rise. *Frontiers in Earth Science*, *3*, 54. https://doi.org/10.3389/feart.2015.00054

Ibarra, D. E., Caves, J. K., Moon, S., Thomas, D. L., Hartmann, J., Chamberlain, C. P., & Maher, K. (2016). Differential weathering of basaltic and granitic catchments from concentration–

discharge relationships. *Geochimica et Cosmochimica Acta*, *190*, 265–293. https://doi.org/10.1016/j.gca.2016.07.006

Ibarra, D. E., Moon, S., Caves, J. K., Chamberlain, C. P., & Maher, K. (2017). Concentration–discharge patterns of weathering products from global rivers. *Acta Geochimica*, *36*(3), 405–409. https://doi.org/10.1007/s11631-017-0177-z

IPCC, (2007). Climate Change 2007: Synthesis Report. Contribution of Working Groups I, II and III to the Fourth Assessment Report of the Intergovernmental Panel on Climate Change Core Writing Team, Pachauri, R.K and Reisinger, A. (Eds.). IPCC, Geneva, Switzerland, 104 pp.

Maher, K. (2011). The role of fluid residence time and topographic scales in determining chemical fluxes from landscapes. *Earth and Planetary Science Letters*, *312*(1–2), 48–58. https://doi.org/10.1016/j.epsl.2011.09.040

Maher, K., & Chamberlain, C. P. (2014). Hydrologic Regulation of Chemical Weathering and the Geologic Carbon Cycle. *New Series*, *343*(6178).

McGuire, K. J., McDonnell, J. J., Weiler, M., Kendall, C., McGlynn, B. L., Welker, J. M., & Seibert, J. (2005). The role of topography on catchment-scale water residence time. *Water Resources Research*, *41*(5), 1–14. https://doi.org/10.1029/2004WR003657

Milner, A. M., Khamis, K., Battin, T. J., Brittain, J. E., Barrand, N. E., Füreder, L., et al. (2017). Glacier shrinkage driving global changes in downstream systems. *Proceedings of the National Academy of Sciences of the United States of America*, *114*(37), 9770–9778. https://doi.org/10.1073/pnas.1619807114

Moon, S., Chamberlain, C. P., & Hilley, G. E. (2014). New estimates of silicate weathering rates and their uncertainties in global rivers. *Geochimica et Cosmochimica Acta*, *134*, 257–274. https://doi.org/10.1016/j.gca.2014.02.033

Neal, E. G., Hood, E., & Smikrud, K. (2010). Contribution of glacier runoff to freshwater discharge into the Gulf of Alaska. *Geophysical Research Letters*, *37*(6), 1–6. https://doi.org/10.1029/2010GL042385

O'Neel, S., Hood, E., Bidlack, A. L., Fleming, S. W., Arimitsu, M. L., Arendt, A., et al. (2015). Icefield-to-ocean linkages across the northern pacific coastal temperate rainforest ecosystem. *BioScience*, *65*(5), 499–512. https://doi.org/10.1093/biosci/biv027

Radić, V., Bliss, A., Beedlow, A. C., Hock, R., Miles, E., & Cogley, J. G. (2014). Regional and global projections of twenty-first century glacier mass changes in response to climate scenarios from global climate models. *Climate Dynamics*, *42*(1–2), 37–58. https://doi.org/10.1007/s00382-013-1719-7

Raiswell, R. (1984). Chemical models of solute acquisition in glacial melt waters. *Journal of Glaciology*, *30*(104), 49–57. https://doi.org/10.1017/S0022143000008480

Raymond, P. A., & Cole, J. J. (2003). *Increase in the Export of Alkalinity from North America's Largest River*. *New Series* (Vol. 301).

RGI Consortium (2017). Randolph Glacier Inventory – A Dataset of Global Glacier Outlines: Version 6.0: Technical Report, Global Land Ice Measurements from Space, Colorado, USA. Digital Media. DOI: https://doi.org/10.7265/N5-RGI-60

Rose, L. A., Karwan, D. L., & Godsey, S. E. (2018). Concentration–discharge relationships describe solute and sediment mobilization, reaction, and transport at event and longer timescales. *Hydrological Processes*, *32*(18), 2829–2844. https://doi.org/10.1002/hyp.13235

Schroth, A. W., Crusius, J., Chever, F., Bostick, B. C., & Rouxel, O. J. (2011). Glacial influence on the geochemistry of riverine iron fluxes to the Gulf of Alaska and effects of deglaciation. *Geophysical Research Letters*, *38*(16), 1–7. https://doi.org/10.1029/2011GL048367

Sharp, M., Tranter, M., Brown, G. H., & Skidmore, M. (1995). Rates of chemical denudation and CO_2 drawdown in a glacier-covered alpine catchment. *Geology*, *23*(1), 61–64. https://doi.org/10.1130/0091-7613(1995)023<0061:ROCDAC>2.3.CO;2

Tadono, T., Ishida, H., Oda, F., Naito, S., Minakawa, K., & Iwamoto, H. (2014). PRECISE GLOBAL DEM GENERATION BY ALOS PRISM. https://doi.org/10.5194/isprsannals-II-4-71-2014

Thornton, M.M., Shrestha, R., Wei, Y., Thornton, P.E., Kao, S., & Wilson, B.E. (2020). Daymet: Daily Surface Weather Data on a 1-km Grid for North America, Version 4. ORNL DAAC, Oak Ridge, Tennessee, USA. https://doi.org/10.3334/ORNLDAAC/1840

Torres, M., Joshua West, A., & Clark, K. E. (2015). Geomorphic regime modulates hydrologic control of chemical weathering in the Andes-Amazon. *Geochimica et Cosmochimica Acta*, *166*, 105–128. https://doi.org/10.1016/j.gca.2015.06.007

Torres, M. A., Moosdorf, N., Hartmann, J., Adkins, J. F., & West, A. J. (2017). Glacial weathering, sulfide oxidation, and global carbon cycle feedbacks. *Proceedings of the National Academy of Sciences of the United States of America*, *114*(33), 8716–8721. https://doi.org/10.1073/pnas.1702953114

Tranter, M., & Wadham, J. L. (2003). Geochemical Weathering in Glacial and Proglacial Environments. *Treatise on Geochemistry*. https://doi.org/10.1016/B0-08-043751-6/05078-7

Walling, D.E., & Webb, B.W. (1983). The dissolved loads of rivers: a global review. In B.W. Webb (Ed), Dissolved loads of rivers and surface water quantity/quality relationships(pp. 3-20). International Association of Hydrological Sciences.

Waldbauer, J. R., & Chamberlain, C.P., (2005). Influence of Uplift, Weathering, and Base Cation Supply on Past and Future CO_2 Levels. *A History of Atmospheric CO_2 and Its Effects on Plants, Animals, and Ecosystems*, (January 2005), 166–184. https://doi.org/10.1007/0-387-27048-5_8

White, A. F., & Blum, A. E. (1995). Effects of climate on chemical weathering in watersheds. *Water-Rock Interaction. Proc. Symposium, Vladivostok, 1995*, *59*(9), 57–60.

White, Art F, Bullen, T. D., Schulz, M. S., Blum, A. E., Huntington, T. G., & Peters, N. E. (2001). *Differential rates of feldspar weathering in granitic regoliths*.

Winnick, M. J., & Maher, K. (2018). Relationships between CO2, thermodynamic limits on silicate weathering, and the strength of the silicate weathering feedback. *Earth and Planetary Science Letters*, *485*, 111–120. https://doi.org/10.1016/j.epsl.2018.01.005

Wymore, A. S., Brereton, R. L., Ibarra, D. E., & Mcdowell, W. H. (2017). Montane Watersheds, 6279–6295. https://doi.org/10.1002/2016WR020016.Received

[Geophysical Research Letters]

Supporting Information for

Concentration-Discharge Patterns Across the Gulf of Alaska Reveal Geomorphological and Glacierization Controls on Stream Water Solute Generation and Export

Jordan Jenckes[1,2] 0000-0002-1811-3076, Daniel E. Ibarra[3] 0000-0002-9980-4599, Lee Ann Munk[1] 0000-0003-2850-545X

[1]University of Alaska Anchorage, Department of Geological Sciences, Anchorage, Alaska 99508, USA

[2]University of Alaska Fairbanks, Department of Geosciences, Fairbanks, Alaska, 99775, USA

[3]Institute at Brown for Environment and Society and the Department of Earth, Environmental and Planetary Science, Brown University, Providence, Rhode Island 02912, USA

Contents of this file

Additional Supporting Information (Files uploaded separately)

Introduction

This supplemental information contains a more complete description of methods, spatial data and tabulated results of statistical analysis and spatial analysis. We also show additional figures mentioned in the main text and two figures which show the regional data of the TDS vs. TSS and HCO_3^- vs. SiO_2. Text S1 explains in more detail the methods used to derive the watershed characteristic. Text S2 explains the methods and results of the Bayesian Information Criterion (BIC) analysis and multiple linear regression.

Text S1.

The physical and climate-based watershed characteristics were calculated in QGIS 3.16.5 and with custom Python scripts. For watershed characteristics derived from raster datasets (elevation statistics, landcover, precipitation, and temperature) we used the Zonal statistics tool within the QGIS Raster analysis toolbox. To calculate watershed characteristics derived from vector data (geology and glacier coverage) a custom Python script was used to clip the input data with each watershed and calculate the percent area each parameter covers within the given watershed. Landcover, geology, and glacier coverage are reported in Table S2 as percent coverage. Climate parameters, mean precipitation and mean temperature, are averages within each watershed calculated from 1981 to 2010 using the DAYMET dataset (Thornton et al., 2020) accessed using Google Earth Engine.

Text S2.

Results of the BIC and multiple linear regression are shown in Table S2. The BIC analysis provides a list of the minimum number of parameters (watershed characteristics) that explain the variation of the given variable (*b*-values and solute yields). The resulting list of parameters are then given to a multiple linear regression (MLR) model. In Table S2 the column "Parameters Chosen" show the parameters used in the MLR along with the sign of the relationship with the given variable in parentheses. For each solute *b*-value and solute yield we provide the R^2 value for the MLR model. We also show what parameters have statistically significant ($p>0.05$) relationships in the final column.

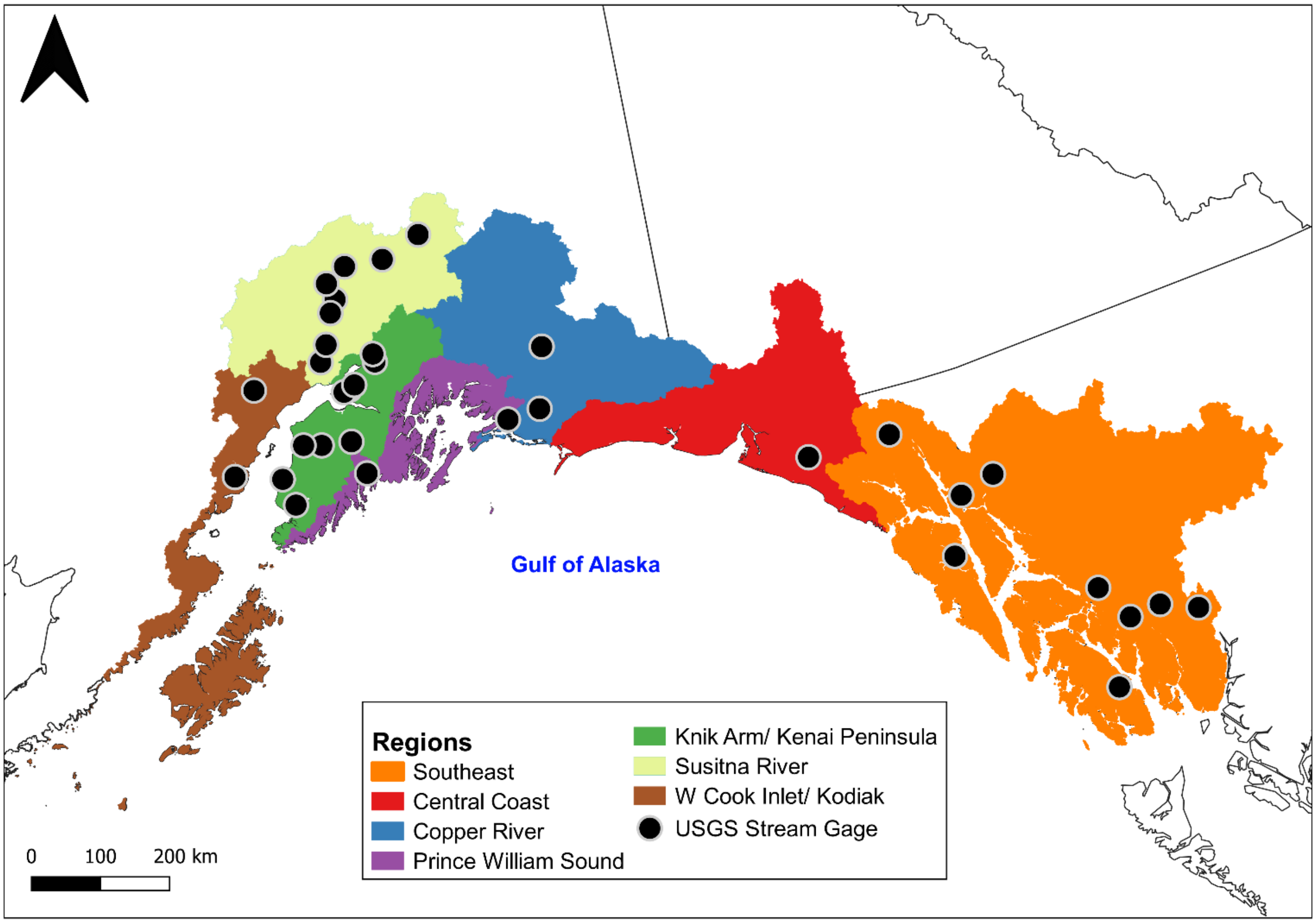

Figure S1. Locations of USGS stream gage sites used for this study. Stream sites were chosen if concentration-discharge measurements equal or exceeded 12 paired measurements. There is a notable lack of stream gages locations within the Central Coast region, likely due to the rugged terrain and abundance of tidewater glaciers.

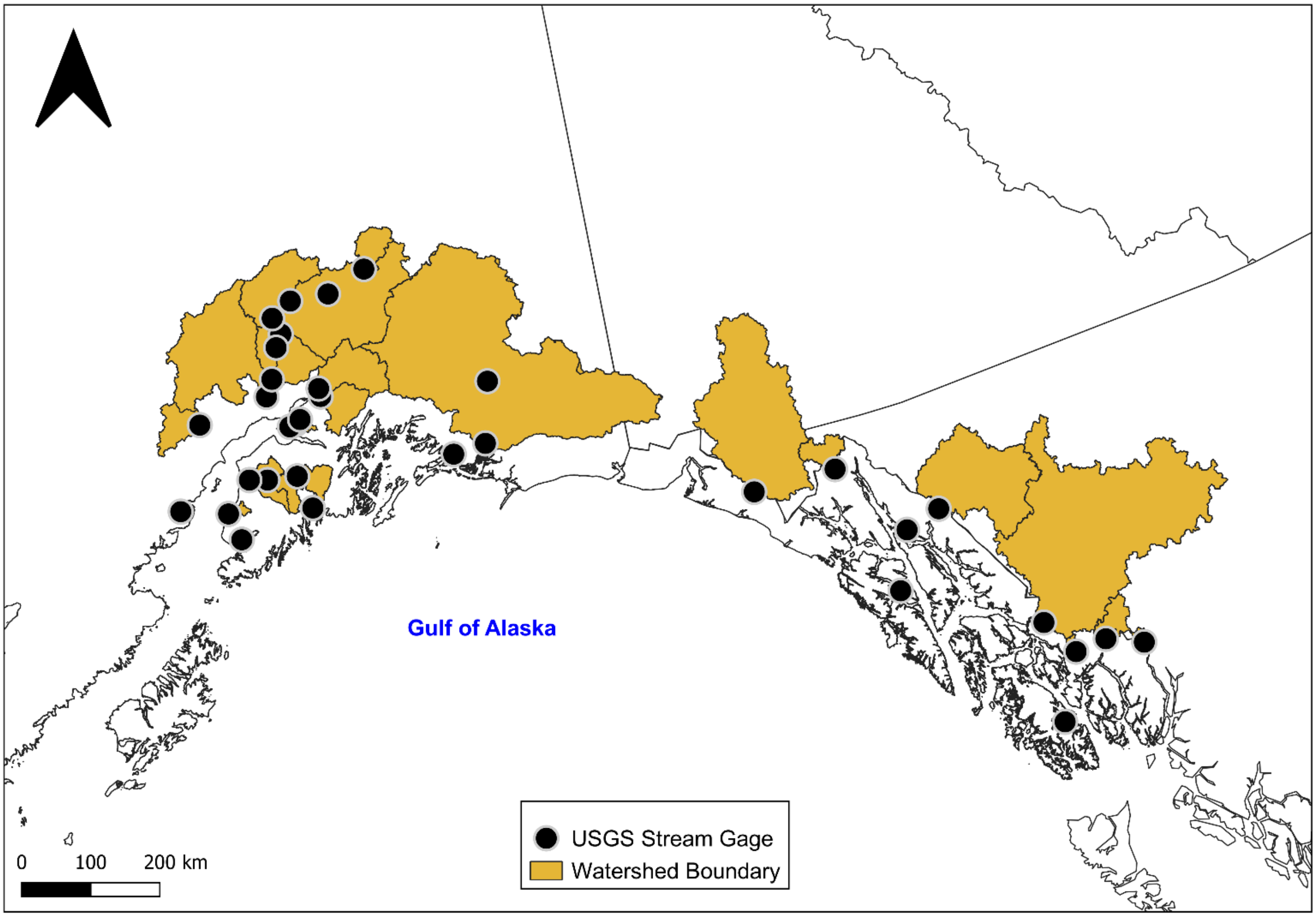

Figure S2. Watershed boundaries used in this study to calculate watershed characteristics along with USGS stream gage sites. Several watersheds within the Susitna River region are nested within each other and do not appear within this map.

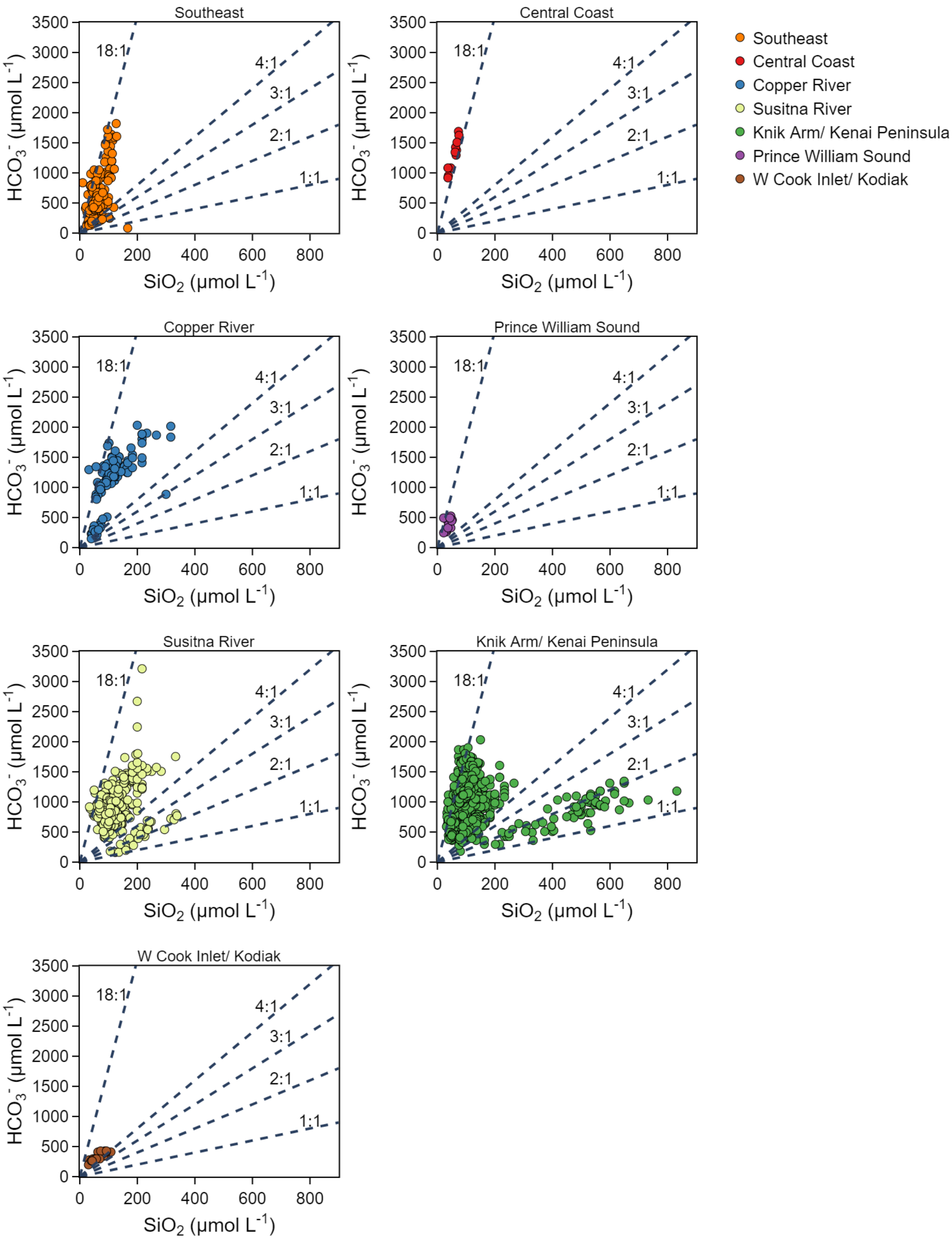

Figure S3. Concentration of HCO_3^- vs. SiO_2 for GoA stream sites plotted by region. Across the various regions of the GoA carbonate dissolution appears to be the primary weathering regime compared to silicate weathering.

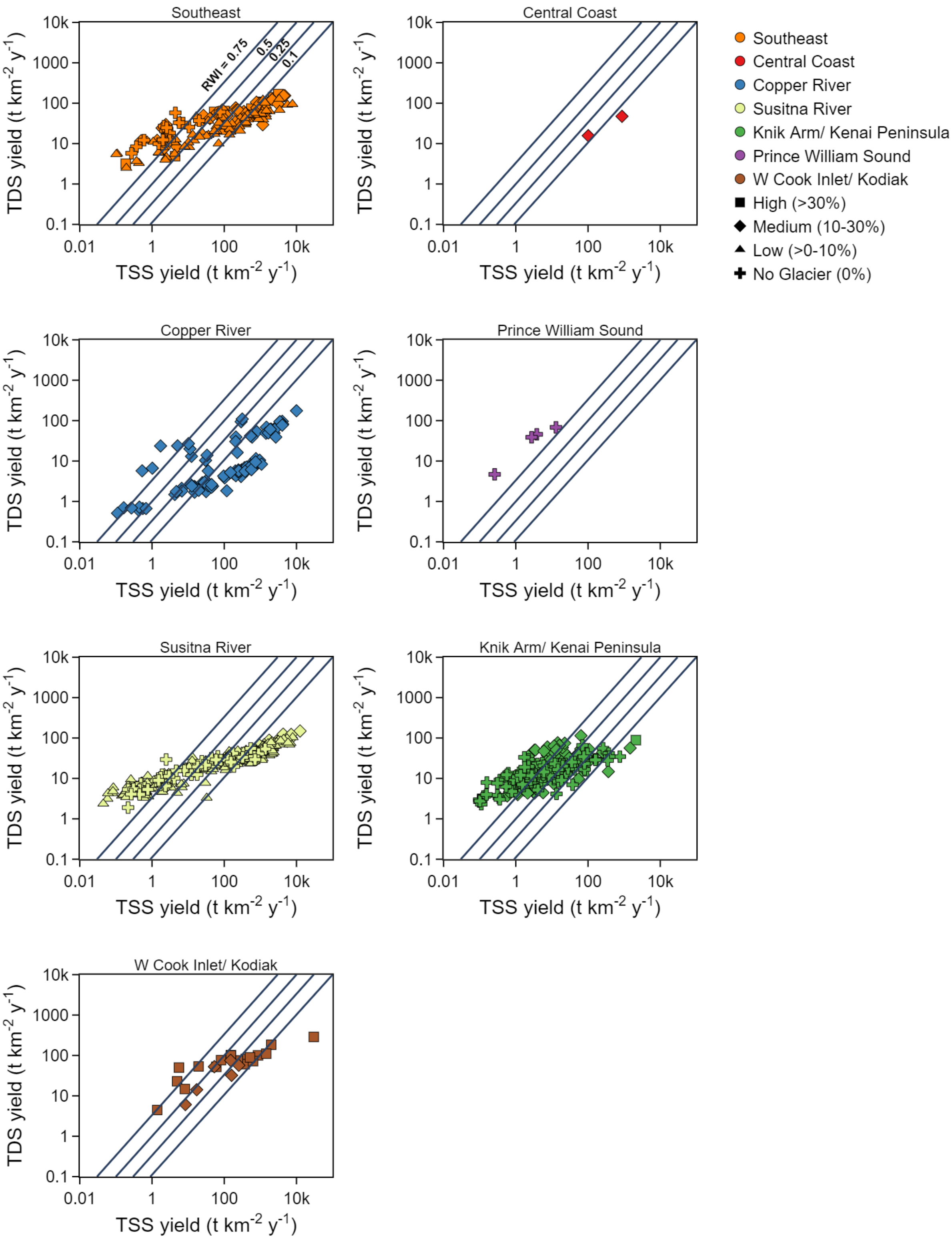

Figure S4. Cross plots of TDS yield vs. TSS yield plotted separately by region. Streams within watersheds with medium to high glacier coverage generally have lower rates of chemical weathering compared to physical weathering. Streams with low to no glacier coverage have higher rates of chemical weathering compared to physical weathering.

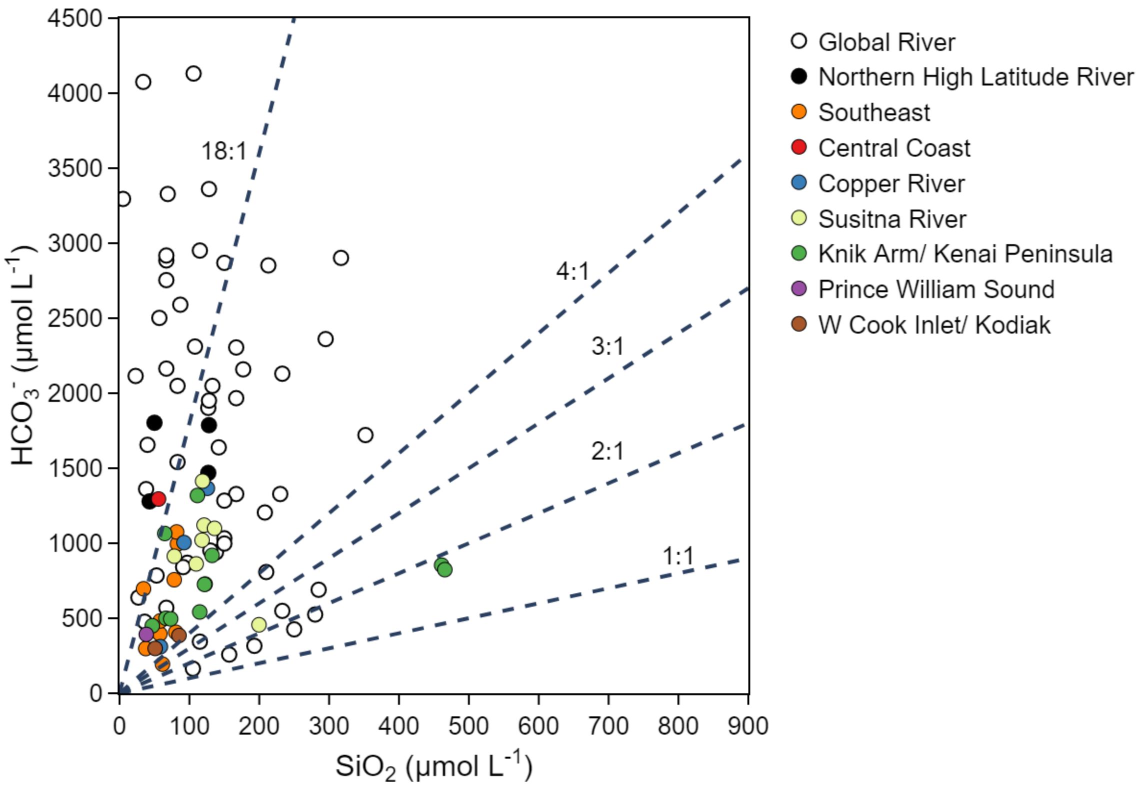

Figure S5. Mean concentration HCO_3^- vs. SiO_2 for GoA streams along with mean global and northern latitude streams. On average GoA streams have lower values compared to the global rivers. Across both datasets carbonate dissolution is the dominate weathering regimes in most basins.

$$CaCO_3(s) + H_2CO_3(aq) \rightleftharpoons Ca^{2+}(aq) + 2HCO_3^-(aq)$$

Equation S1. Carbonation of calcite resulting in 1:0.5 molar ratio of HCO_3^-: Ca^{2+}.

Solute b-value	Parameters for min. BIC	R^2	Parameters Chosen	$p<0.05$
HCO_3^-	4	0.2375	Relief (+), Wetland (-)	Wetland
Ca^{2+}	3	0.3488	Mean Aspect (+), Mean Slope (+), Relief (+)	All but Relief
Mg^{2+}	2	0.3423	Mean Aspect(+), Mean Slope (+)	All
Na^+	2	0.2825	Mean Aspect (+), Relief (+)	Only Relief
SiO_2	5	0.6153	Glacier Coverage (+), Mean Slope (+), Mean Elevation (-), Barren lands(+), Putonic (-), Mean q ($m^3/s/km^2$) (-)	All
TSS	8	0.9296	Mean Precip. (+), Mean Temp(+), Metamorphic (-), Volcanic (+), Mean Elevation (+), Shrubland (+), Wetland (+), Mean q ($m^3/s/km^2$) (+)	All but Mean Precip.
Solute Yield	**Parameters for min. BIC**	**R^2**	**Parameters Chosen**	**$p<0.05$**
HCO_3^-	2	0.4784	Glacier Coverage (+), Plutonic (-)	All
Ca^{2+}	2	0.5198	Glacier Coverage (+), Plutonic (-)	All
Mg^{2+}	2	0.4995	Glacier Coverage (+), Plutonic (-)	All
Na^+	3	0.4700	Glacier Coverage (+), Plutonic (-), Grassland (-)	All but Plutonic
SiO_2	3	0.4848	Basin Area (km^2) (-), Glacier Coverage (+), Plutonic (-)	All
TSS	4	0.5860	Glacier Coverage (+), Plutonic (+), Volcanic (+), Barren Lands (-),	Glacier Coverage and Barren Lands

Table S1. Results of the BIC analysis and multiple linear regression. The variation of the *b*-values is primarily explained by mean aspect, slope and relief. The solute yields are mainly controlled by glacier coverage. The signs within the parentheses indicate if the given variable has a positive or negative relationship with the given parameter.

Table S2. The table provides all the input data for the BIC and multiple linear regression analysis. This includes the used watershed characteristics and mean temperature and precipitation. Also included are the calculated *b*-values and yields for each solute used in the analysis.

Dataset S1. Includes three shapefiles for the USGS watershed boundaries and USGS stream sites used in this study, and the regional boundaries of the GoA.